Universal Evolution of Perfect Lenses

W. H. Wee and J. B. Pendry
Blackett Laboratory, Imperial College London SW7 2AZ, United Kingdom
(Received 10 February 2011; published 21 April 2011)

This Letter is a theoretical attempt to answer two questions. First how long does it takes for perfect lensing to be observed, and second how does loss diminish the performance of a *general* perfect lens. The method described in this Letter is universal, in the sense that it can be applied to perfect lenses of any arbitrary geometry. We shall show that the dynamics of perfect lensing is equivalent to the dynamics of 2 coupled simple harmonic oscillators. Moreover we shall derive quantitatively, the effects of losses on a compact perfect lens.

DOI: 10.1103/PhysRevLett.106.165503 PACS numbers: 81.05.Xj, 42.25.Bs

In 2000, Pendry realized that a slab of material with $\epsilon = \mu = -1$ would act as a "perfect lens," enabling in principle, images with unlimited resolution [1]. The power of the perfect lens over conventional lenses, lies in its ability to focus not only the light rays but also the evanescent near fields. With the advent of transformation optics [2], this simple slab lens could be generalized to lenses of arbitrary geometry, further expanding the power of the perfect lens. For instance, besides enhanced resolution, lenses with compact geometry (compact perfect lenses), can "supermagnify" objects embedded within to a size much larger than the physical dimension of the lens [3]. Undoubtedly, the richness of the perfect lens has open up many new applications previously inaccessible to conventional optics. These range from subwavelength imaging [4], strongly enhanced scattering [5,6], enhanced directivity of antennas [7] and even cloaking "at a distance" [8] and casting optical illusions [9]. While these and many other applications are fascinating, most if not all, the current applications in literature are based on steady state. In reality "perfect lensing" takes time to develop, hence it is natural to ask the following: "How long does this take?" and "What are the effects of losses?" While these were answered before by [10–12], the solutions obtained mainly apply to the flat perfect lens. In view of this and the richness of the general perfect lens, we derive a more general method applicable to lenses of any arbitrary geometry.

Since we are interested in the time evolution of the compact perfect lens, we can broadly divide the space into three regions denoted by $I = 1, 2$ and 3, corresponding to the space outside, within, and enclosed by the lens [Fig. 1(a)]. Quantities Q (fields and permeabilities, etc.) in a specific region I are denoted by Q_I. For our model, we shall assume that region 1 is vacuum and region 3 is designed to look transparent. To study the time evolution we begin from Maxwell's equation in frequency domain,

$$\nabla \times \mathbf{E}_I = -i\omega \boldsymbol{\mu}_I \cdot \mathbf{H}_I \qquad \nabla \times \mathbf{H} = i\omega \boldsymbol{\epsilon}_I \cdot \mathbf{E}_I \quad (1)$$

where $\boldsymbol{\epsilon}_I(\omega)$, $\boldsymbol{\mu}_I(\omega)$ is the permittivity and permeability in region I. Here the physical content of the evolution is captured by the frequency dispersion of $\boldsymbol{\epsilon}_2(\omega)$, $\boldsymbol{\mu}_2(\omega)$. For simplicity let us assume that $\boldsymbol{\epsilon}_2(\omega, \mathbf{x}) = \boldsymbol{\mu}_2(\omega, \mathbf{x})$, and

$$\boldsymbol{\epsilon}_2(\omega, \mathbf{x}) = \Gamma(\omega, \mathbf{x}) \cdot \hat{\boldsymbol{\epsilon}}_2(\mathbf{x}) \quad (2)$$

where $\hat{\boldsymbol{\epsilon}}_2(\mathbf{x})$ is the permittivity of the lossless perfect lens. $\Gamma(\omega, \mathbf{x})$ is a function which captures the temporal dispersion of the permittivity. At the working frequency ($\omega = \omega_0$) of the lens, $\Gamma(\omega_0, \mathbf{x}) = 1$. Assuming that the temporal dispersion is slowly varying with space ($\Gamma(\omega, \mathbf{x}) \approx \Gamma(\omega)$), and for small frequency deviation ($\omega = \omega_0 + \delta\omega$), we can expand this to first order, as $\Gamma(\omega) \approx (1 + \gamma)$, where $\gamma = \delta\omega \cdot \frac{\partial \Gamma(\omega_0)}{\partial \omega} = \delta\omega \cdot \dot{\Gamma}(\omega_0)$ [henceforth overdots imply a derivative, i.e., $\dot{Q}(\zeta) = \partial_\zeta Q(\zeta)$]. Effects of losses can also be included by allowing γ to be complex; $\gamma = (\omega - \omega_0) \cdot \dot{\Gamma}(\omega_0) - i\sigma$; where $\sigma \geq 0$ is the loss tangent.

In general the solution of the fields for the outermost region is simple, since $\epsilon_1 = \mu_1 = 1$ (for some geometries, these have well-known solutions). In contrast, the fields within the lens generally are not easily solved. A perfect lens with an arbitrary geometry may have a complicated permittivity or permeability that is both anisotropic and a

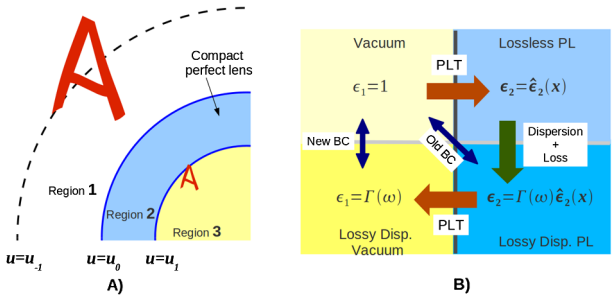

FIG. 1 (color online). (a) Figure of a compact perfect lens. Here the embedded object and its enlarged image is denoted by the red font "A." (b) Schematic of the simplification of BCs. The various quadrants represents the type of materials involved. The complex BC of a lossy dispersive perfect lens is translated to a simplified BC with a "lossy dispersive vacuum."

varying function of space $[\boldsymbol{\epsilon}_2(\omega, \mathbf{x}), \boldsymbol{\mu}_2(\omega, \mathbf{x})]$, making the solution of the fields within the lens highly nontrivial. This is further complicated if we consider effects of temporal dispersion and losses.

Fortunately this difficulty can be circumvented if we make use of the symmetry properties of the field solutions imposed by the perfect lens theorem (PLT) [3]. PLT states that, a perfect lens can be viewed as an optical construct, where fields within the lens (region 2) are a mirror copy of the fields in the space (region 1) that the lens was designed to see through. This implies that the complicated fields within region 2 can be represented by its simpler image fields in region 1. (These pair of fields or space are referred to as *complementary*). This association of complementary fields therefore implies that complicated boundary conditions at the interface between region 2 and 3 can now be translated to simpler boundary conditions embedded in region 1. [See Fig. 1(b)]

Now the deviation of the permittivity (permeability) $\boldsymbol{\epsilon}_2(\omega, \mathbf{x})$ from $\hat{\boldsymbol{\epsilon}}_2(\mathbf{x})$ means that the fields in region 2 are no longer complementary to vacuum in region 1; rather it would be complementary to a "lossy dispersive material" given by PLT to be:

$$\boldsymbol{\epsilon}_1(\omega, \mathbf{x}) = \boldsymbol{\mu}_1(\omega, \mathbf{x}) \approx (1 + \gamma). \tag{3}$$

It is important to note that the permittivity given above in (3) is still spatially invariant hence simpler to deal with than (2). If we solved for the E field solution in region 1, for some general set of coordinates given by $\{u, v, w\}$, these can be written as a sum of eigenmodes where the m eigenmode is given by $f_m^{\pm}(\gamma|u)$; the "+" and "−," denote the forward and backward waves, respectively; the first argument indicates that these fields are propagating a material given by (3), and the second set of arguments are the coordinates (where u is the only variable, v, w are constant). In this coordinate system, $u = u_j$ (for some constant u_j; $j = \pm 1, 0$) corresponds to the boundaries of the lens—u_0 and u_1 corresponds to the inner and outer surface, and u_{-1} to the image plane or complementary surface to u_1. Applying the PLT, we then get the following simplified boundary conditions (BCs):

$$\begin{pmatrix} f_m^+(0|0) & f_m^-(0|0) \\ f_m^{+\prime}(0|0) & f_m^{-\prime}(0|0) \end{pmatrix}_{\parallel} \cdot \begin{pmatrix} 1 \\ R_m \end{pmatrix} = \begin{pmatrix} f_m^+(\gamma|0) & f_m^-(\gamma|0) \\ f_m^{+\prime}(\gamma|0) & f_m^{-\prime}(\gamma|0) \end{pmatrix}_{\parallel} \cdot \begin{pmatrix} c_m \\ b_m \end{pmatrix}, \qquad u = u_0$$
$$\begin{pmatrix} f_m^+(\gamma|-1) & f_m^-(\gamma|-1) \\ f_m^{+\prime}(\gamma|-1) & f_m^{-\prime}(\gamma|-1) \end{pmatrix}_{\parallel} \cdot \begin{pmatrix} c_m \\ b_m \end{pmatrix} = \begin{pmatrix} f_m^+(0|-1) & f_m^-(0|-1) \\ f_m^{+\prime}(0|-1) & f_m^{-\prime}(0|-1) \end{pmatrix}_{\parallel} \cdot \begin{pmatrix} T_m \\ 0 \end{pmatrix}, \qquad u = u_1 \tag{4}$$

where the arguments u_0 and u_{-1} are replaced by numbers 0 and -1, respectively, for concision. The first rows of the matrices in (4) are the E fields while the second are the H fields [from (1)]—thus the primed superscript indicates $f_m^{\pm\prime} = -\boldsymbol{\mu}^{-1} \cdot \nabla \times (f_m^{\pm})$. The $\parallel$ sign in the subscript indicates that each element of the matrix is projected onto the u surface. For simplicity we shall assume this projection and drop this sign. The elements of the column vectors, T_m, R_m are the transmission and reflection coefficients for the m eigenmode, while c_m, b_m are the outgoing and incoming eigenmodes within the lens. Note in the simplified BC, everything is written in terms of known solutions embedded in region 1.

Now assuming small γ, and retaining the lowest order terms, we can solve (4) for T_m and R_m as:

$$T_m(\omega) \approx \frac{1}{\Delta_m}(C_{-1}^{-+}(0)C_0^{+-}(0))$$
$$R_m(\omega) \approx \frac{1}{\Delta_m}(\dot{C}_0^{++}(0)C_{-1}^{-+}(0) - C_0^{-+}(0)\dot{C}_{-1}^{++}(0))\gamma \tag{5}$$

where $\Delta_m(\omega) \approx C_{-1}^{-+}(0)C_0^{+-}(0) - \dot{C}_{-1}^{++}(0)\dot{C}_0^{--}(0)\gamma^2$, here the various functions C_i are given by: $C_i^{\pm\pm}(\gamma) = [f_m^{\pm}(\gamma|i), f_m^{\pm}(0|i)]$ (for $i = 0, -1$); the square brackets imply $[a, b] = ab' - ba'$. It is easy to check for $\sigma = 0$, then $T_m(\omega_0) = 1$, $R_m(\omega_0) = 0$, which corresponds to lossless perfect lensing as expected.

Now, all the physics is captured by the analytic structure of these transmission and reflection coefficients. Since the poles of $T_m(\omega)$ and $R_m(\omega)$, are given by the simple zeros of $\Delta_m(\omega)$ which is quadratic in ω, there are two (complex) poles given by $\omega_{m\pm} = \omega_0 \pm \eta_m + i\hat{\sigma}$ where $\hat{\sigma} = \sigma/\dot{\Gamma}(\omega_0)$ and

$$\eta_m^2 = \frac{1}{\dot{\Gamma}(\omega_0)^2} \cdot \frac{C_{-1}^{-+}(0)C_0^{+-}(0)}{\dot{C}_{-1}^{++}(0)\dot{C}_0^{--}(0)}. \tag{6}$$

The $\Re(\omega_{m\pm})$ therefore, corresponds to the resonant frequency of the lens, where the "+" and "−" subscripts refer to the higher frequency antisymmetric (ASPP) and lower frequency symmetric (SSPP) surface plasmon polariton modes, respectively. Thus, η_m can be understood to be the coupling strength between these modes.

Now (5) strictly holds for $T_m(\omega)$ for positive ω. We can analytically continue this for negative ω if we take into account that T_m, R_m as a function of time are real (the reality condition)—that is $T_m(\omega) = T_m^*(-\omega)$, etc. Hence the full T_m should be $T_m(\omega) \sim 1/[(\omega - \omega_{m-}) \times (\omega - \omega_{m+})(\omega + \omega_{m-}^*)(\omega + \omega_{m+}^*)]$ where the first two poles are for positive ω and the latter two are added on for negative ω. We can similarly impose reality on $R_m(\omega)$ and get the following coefficients:

$$T_m(\omega) = -(2\omega_0\bar{\eta}_m)^2 \cdot \frac{1}{[(\omega_0^2-\omega^2)+2\omega_0\bar{\eta}_m+2i\omega\hat{\sigma}][(\omega_0^2-\omega^2)-2\omega_0\bar{\eta}_m+2i\omega\hat{\sigma}]}$$
$$R_m(\omega) = 2\omega_0\bar{\eta}_{m,1} \cdot \frac{(\omega^2-\omega_0^2)}{[(\omega_0^2-\omega^2)+2\omega_0\bar{\eta}_m+2i\omega\hat{\sigma}][(\omega_0^2-\omega^2)-2\omega_0\bar{\eta}_m+2i\omega\hat{\sigma}]} \quad (7)$$

where all the "barred" complex quantities are defined as $\bar{\eta}_m = \Re(\eta_m) + i \cdot \frac{\omega}{\omega_0}\Im(\eta_m)$. The constant prefactor $\eta_{m,1}$ in front of the zeros and poles is added on to satisfy the condition that T_m, R_m in (7) are equivalent to the $T_m(\omega > 0)$ $R_m(\omega > 0)$ [Eq. (5) for $\omega \sim \omega_0$].

If we do a time domain Fourier transform on (7) (replacing $i\omega$ with ∂_t), and make the following correspondence:

$$x_l \rightarrow E_{\text{ref.}}(u = u_{-1}, \omega)$$
$$x_r \rightarrow \frac{\bar{\eta}_{m,1}}{\bar{\eta}_m} E_{\text{trans.}}(u = u_1, \omega) \quad (8)$$
$$f \rightarrow 2\omega_0\bar{\eta}_{m,1} E_{\text{inc.}}(u = u_{-1}, \omega);$$

the dynamics of a perfect lens is then equivalent to

$$\ddot{x}_l + 2\hat{\sigma}\cdot\dot{x}_l + \omega_0^2 x_l - 2\omega_0\Re(\eta_m)x_r - 2\Im(\eta_m)\dot{x}_r = f$$
$$\ddot{x}_r + 2\hat{\sigma}\cdot\dot{x}_r + \omega_0^2 x_r - 2\omega_0\Re(\eta_m)x_l - 2\Im(\eta_m)\dot{x}_l = 0, \quad (9)$$

which is the equation of motion for a system of 2 coupled simple harmonic oscillators each with a natural frequency of $\omega = \omega_0$ (see Fig. 2). For large m, the fields are predominantly evanescent hence $\eta_m \sim \Re(\eta_m)$ (since all C_i would be real) and we can ignore the velocity dependent coupling in (9). One can then easily see that (9) is exactly equivalent to Gomez-Santos' analysis of the flat perfect lens [11].

Now the time evolution of the perfect lens can be easily obtained from (9). When the incident electric field $E_{\text{inc.}}(u = u_{-1}, t) = \Theta(t)e^{i\omega_0 t}$ the transmitted electric field

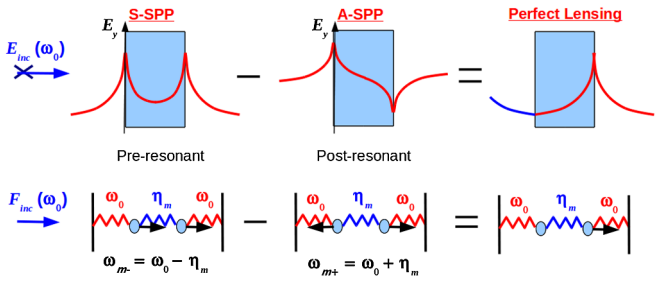

FIG. 2 (color online). Analogy between the perfect lens and its mechanical analogue. An incident field at ω_0 would excite both the SSPP and ASPP normal modes (with natural frequencies given by ω_{m-} and ω_{m+}) equally. The superposition of these modes would result in a perfect reflectionless transmission [$R_m(\omega_0) = 0$, $T_m(\omega_0) = 1$].

will be given by: $E_{\text{trans.}}(t) = A(t)e^{i\omega_0 t} + \text{c}\cdot\text{c}$, where the envelope function $A(t)$ (for large m) is given by:

$$A(t) \simeq \left(\frac{\eta_m^2}{(\eta_m^2+\hat{\sigma}^2)}\right)[1-\cos(\eta_m t)\exp(-\hat{\sigma}t)] \quad (10)$$

where the term in the first bracket is the steady state solution (as $t \rightarrow \infty$) [equivalent to the transmission coefficient $T_m(\omega_0)$] and the second term in the second bracket is the transient term, a consequence of the beating between the $\omega_{m\pm}$ normal modes.

The time it takes for an m eigenmode to be established is inversely proportional to the coupling strength, $t_m \sim 1/\eta_m$. Since η_m tends to fall off for larger m, this implies that these larger m eigenmodes take a longer time to be established. Consequently, since the smallest feature the lens can resolve is $\Delta x \sim 1/m$, this means the higher resolution would take a much longer time to be developed. In principle, knowing η_m would tell us how long we have to wait before the lens operates at a level where we can see what we want to see. Consequently we can reduce this lag time by selecting materials with smaller dispersion. In addition with Eq. (10) we can also derive a criterion to determine when losses would dominate and kill the perfect lensing effect. This would occur when the denominator term is dominated by losses—when $\sigma > \dot{\Gamma}(\omega_0)\eta_m$. Substituting (6) into this criterion, we can define a critical loss σ_m:

$$\sigma_m^2 = \dot{\Gamma}(\omega_0)^2\eta_m^2 = \left|\frac{C_{-1}^{-+}(0)C_0^{+-}(0)}{\dot{C}_{-1}^{++}(0)\dot{C}_0^{--}(0)}\right| \quad (11)$$

where any loss $\sigma > \sigma_m$ would block the transmission of that m eigenmode. Since σ_m is a monotonically decreasing function with respect to m, Eq. (11) also tells us the largest m eigenmode that can be transmitted through—the largest $m = m_c$ satisfying $\sigma_m > \sigma$; m_c in turn would determine the best resolution possible.

We can now compare our results with previous work on the time evolution of the flat perfect lens. The obvious coordinate system to use is the Cartesian, $\{u, v, w\} = \{x, y, z\}$, where $u_{\pm 1} = \pm d$, $u_0 = 0$. For TM polarization the E field eigenmodes given by $f_m^{\pm}(\gamma|u) = \exp(\mp k_z z)\hat{\mathbf{y}}$ where $k_z = \sqrt{m^2 - \epsilon(\omega)\mu(\omega)\cdot\omega^2/c^2}$ with $\epsilon(\omega) = 1+\gamma$. Substituting this into (6) we get (for large m), $\eta_m \sim 2(\dot{\Gamma}(\omega_0)^{-1}\exp(-md))$, exactly the same as the coupling strength in [11]. Similarly from (11), the critical loss is $\sigma_m \approx 2\exp(md)$, which tells us that for losses given by σ, $m_c \sim \ln(\sigma/2)/d$. Since the limit of image resolution is

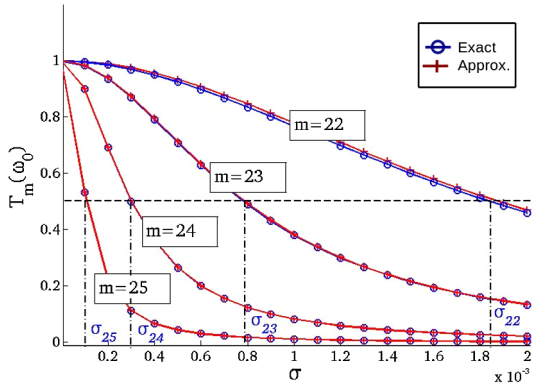

FIG. 3 (color online). Graph of transmission coefficient $T_m(\omega_0)$ as a function of loss σ for the cylindrical perfect lens. The curves are for various m eigenmodes (labeled inset). Here we can see that there is an excellent agreement between numerics and the approximation [using (5)]. The critical losses σ_m denoted in the graph, are given by the values of σ where $T_m(\omega_0) = 0.5$.

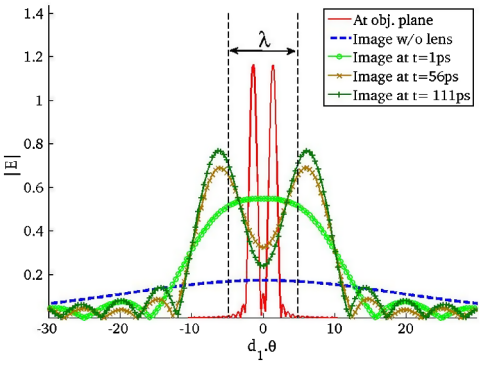

FIG. 4 (color online). Time evolution of an image ($|E|$ field) using a cylindrical perfect lens (losses, $\sigma = 1.8 \times 10^{-3}$). The object is a subwavelength ($\lambda/3$) double slit. Without the lens, the slits are not resolved. With the lens and enough time (~ 60 ps; calculation based on the fishnet structure [13]), a clearly *resolved* and *magnified* ($4\times$) image is formed.

given by $\Delta x \sim 2\pi/m_c$ we can therefore show that for the slab lens $\Delta x \sim d/[2\pi \cdot \ln(\sigma/2)]$ as derived by Smith *et al.* [10] and Merlin [12].

For the cylindrical perfect lens, the obvious coordinate system to use is the cylindrical polar, $\{u, v, w\} = \{r, \theta, z\}$, where $u_{-1} = d_1$, $u_0 = d_2$ and $u_1 = d_3$ with $d_1 > d_2 > d_3$. For TE polarization the E field eigenmodes given by $f_m^-(\gamma|u) = H_m^{(1)}(kr)e^{im\phi}\hat{\mathbf{z}}$ and $f_m^+(\gamma|u) = J_m(kr)e^{im\phi}\hat{\mathbf{z}}$, where $k = \sqrt{\epsilon(\omega)\mu(\omega)}\omega/c$ with $\epsilon = \mu = 1 + \gamma$. Substituting these into (11), we get

$$\sigma_m^2 = \frac{(k_0^2 d_1 d_2)^2}{[\dot{J}_m(k_0 d_1), J_m(k_0 d_1)][H_m^{(1)}(k_0 d_2), \dot{H}_m^{(1)}(k_0 d_2)]} \quad (12)$$

This result can be easily compared with numerical simulations of $T_m(\omega_0)$ as a function of loss σ (Fig. 3), for a cylindrical lens with outer and inner diameter given by $d_2 = 20$, $d_3 = 10$, respectively (the image would be magnified by $d_1/d_3 = 4\times$). First we note that as asserted, losses affect the transmission of larger m eigenmodes more. Second, as an example, we can see from Fig. 3 that for $\sigma \sim 1.8 \times 10^{-3}$, $m_c = 22$. This translates to an angular resolution of $\Delta\theta = 2\pi/m_c$ or $\Delta x \sim \lambda/3$. Together with its inherent magnification, this means that a subwavelength object with size $\lambda/3$ would cast a wavelength size ($4 \times \lambda/3$) image (Fig. 4) enabling it to be visible in the far field. Such an image would take roughly $\sim$60 ps to be formed (calculation based on fishnet structure at $\omega_0 = 170$ THz [13]).

In conclusion we have shown the analogy between a general perfect lens with a set of coupled oscillators. From this, we have a quantitative description of the mechanics of the perfect lens, enabling us to determine how losses affect the perfect lens. We can also determine the time required for a particular resolution to occur, which is important in sensing applications. In particular we can decrease this delay by designing metamaterials with smaller dispersion. Finally this formulation is *universal* in the sense that it does not depend on the details of the lens.

[1] J. B. Pendry, Phys. Rev. Lett. **85**, 3966 (2000).
[2] J. B. Pendry, D. Shurig, and D. R. Smith, Science **312**, 1780 (2006).
[3] J. B. Pendry and S. A. Ramakrishna, J. Phys. Condens. Matter **15**, 6345 (2003).
[4] N. Fang, H. Lee, Sun Cheng, and X. Zhang, Science **308**, 534 (2005).
[5] W. H. Wee and J. B. Pendry, New J. Phys. **11**, 073033 (2009).
[6] Tao Yang, Huanyang Chen, Xudong Luo, and Hongru Ma, Opt. Express **16**, 18545 (2008).
[7] W. H. Wee and J. B. Pendry, New J. Phys. **12**, 033047 (2010).
[8] Yun Lai, Huanyang Chen, Zhao-Qing Zhang, and C. T. Chan, Phys. Rev. Lett. **102**, 093901 (2009).
[9] Y. Lai, J. Ng, H. Y. Chen, D. Z. Han, J. J. XiaoZ.-Q. Zhang, and C. T. Chan, Phys. Rev. Lett. **102**, 253902 (2009).
[10] D. R. Smith, D. Schurig, M. Rosenbluth, S. Schultz, S. A. Ramakrishna, and J. B. Pendry, Appl. Phys. Lett. **82**, 1506 (2003).
[11] G. Gomez-Santos, Phys. Rev. Lett. **90**, 077401 (2003).
[12] R. Merlin, Appl. Phys. Lett. **84**, 1290 (2004).
[13] J. Valentine, S. Zhang, T. Zentgraf, E. Ulin-Avila, D. A. Genov, G. Bartal, and X. Zhang, Nature (London) **455**, 376 (2008).